Arch. Pharm. Res.
DOI 10.1007/s12272-015-0699-z

Archives of Pharmacal Research
www.springer.com/12272

RESEARCH ARTICLE

Synthesis, biological evaluation, drug-likeness, and *in silico* screening of novel benzylidene-hydrazone analogues as small molecule anticancer agents

Mohammad Sayed Alam[1,2] · **Dong-Ung Lee**[1]

Received: 3 October 2015 / Accepted: 12 December 2015

Abstract A series of fifteen benzylidene-hydrazone analogues (**3a–o**), including eight new compounds, were synthesized and evaluated for their cytotoxic activities in four human cancer cell lines and for their antioxidant activities using DPPH. Of the tested compounds **3e**, which possesses two methoxy substituents in its benzylidene phenyl ring, was found to be potently cytotoxic to all cancer cell lines tested with IC_{50} values of 0.12 (lung), 0.024 (ovarian), 0.097 (melanoma), and 0.05 μM (colon), and these IC_{50} values were comparable to those of the doxorubicin standard ($IC_{50} = 0.021$, 0.074, 0.001, and 0.872 μM, respectively). DPPH assay showed compounds **3f, 3i**, and **3g** had IC_{50} values of 0.60, 0.99, and 1.30 μM, respectively, which were comparable to that of ascorbic acid ($IC_{50} = 0.87$ μM). Computational parameters such as, drug-likeness, ADME properties, toxicity effects, and drug scores were evaluated, and none of the fifteen compounds violated Lipinski's rule of five or Veber's rule, and thus they demonstrated good drug-likeness properties. In addition, all fifteen compounds had a higher drug score than the doxorubicin and BIBR1532. *In silico* screening was also conducted by docking of the active compounds on the active site of telomerase reverse transcriptase catalytic subunit, an important therapeutic target of anticancer agents, to determine the probable binding properties. The total binding energies of docked compounds are correlated well with cytotoxic potencies (pIC_{50}) against lung, ovarian, melanoma, and colon cancer cell lines indicating that the benzylidene-hydrazones could use for the development of new anticancer agents as a telomerase inhibitor.

Keywords Benzylidene-hydrazones · Antitumor agents · Antioxidant · Drug-likeness · *In silico* screening · Molecular modelling

Introduction

The most common cancers, such as, those of the lung, breast, colorectum, stomach, liver, and skin, are a major global health concern (Seigel et al. 2015). Chemotherapy is most widely used cancer treatment, but is associated with serious side effects and other problems, for example, the drugs used interact with unnecessary binding sites, their selectivities and efficacies are limited, and their effectiveness are sometimes undermined by the development of drug resistance. Furthermore, cancer growth and metastasis are driven by multiple pathways. For these reasons, the discovery of new, multi-targeting anticancer agents is of critical importance.

In vivo oxidative stress produces free radical species (ROS), which can oxidize many biomolecules, and are causally associated with several diseases, such as, cancer, Alzheimer's disease (AD), metabolic disorders, cellular aging, reperfusion damage, and inflammatory diseases. Anti-oxidants are administered to prevent the formation or to neutralize free radicals and to enable repair of the damage caused (Sun-Waterhouse et al. 2009), and thus, importantly provide protection from the developments of such diseases.

Electronic supplementary material The online version of this article (doi:10.1007/s12272-015-0699-z) contains supplementary material, which is available to authorized users.

✉ Dong-Ung Lee
dulee@dongguk.ac.kr

[1] Division of Bioscience, Dongguk University, Gyeongju 780-714, Republic of Korea

[2] Department of Chemistry, Jagannath University, Dhaka 1100, Bangladesh

Published online: 23 December 2015

Hydrazones are used as building blocks for the syntheses of a variety of useful bioactive compounds, and are characterized by the presence of a open chain –RR_1-NN=CR_2R_3-group. Furthermore, hydrazones exhibit a broad range of biological activities, such as, anticancer (Zheng et al. 2009), antibacterial (Rasras et al. 2010), anti-tuberculosis (Hearn et al. 2009), anti-convalescent (Jain et al. 2007), anti-oxidant (Anouar 2014), and diuretic properties (Mishra et al. 1995; Supuran et al. 1996), and have been used as herbicides, insecticides, nematocides, rodenticides, plant growth regulators, and as housefly sterilants (Mohan et al. 1988; Akelah et al. 1993). The wide ranging biochemical activities and uses of hydrazone analogues have attracted considerable research attention. As part of our continued search for novel bioactive compounds (Alam et al. 2011, 2012, 2013) and the results of literature survey, we synthesized a series of small molecule benzylidene-hydrazone analogues with pharmacodynamic scaffolds and anticancer properties similar to those of telomerase inhibitors (Fig. 1). Telomerase, a unique ribonucleoprotein enzyme, is a potential therapeutic target for several structurally diverse anticancer agents (Tian et al. 2010; Read et al. 2001; Moorthy et al. 2012; Luo et al. 2013; Xing et al. 2014). Literature survey revealed that some telomerase inhibitors possessing amide (–NHCO–) and azomethine (–C=N–) functional group to exhibit telomerase inhibitor activity, and they are also abundantly observed in pharmaceutically active compounds as a prominent structural motif. For instance, BIBR1532 (Fig. 1a), an amide derivative of 3-(naphthalene-2-yl)but-2-enoic acid, is a promising human telomerase reverse transcriptase (hTERT) inhibitor so far (Tian et al. 2010). It exerts its anticancer activity through the specific blocking of DNA elongation and thereby, acts as a non-competitive telomerase inhibitor (Pascolo et al. 2002). Benzylidene-hydrazone analogues in the present study also possess amide and azomethine structural motif including polar and non-polar substituents in the phenyl rings, and they might involve in hydrogen bond formation and hydrophobic interactions with targeting protein or DNA to exert cell proliferation inhibition activity (Tian et al. 2010). Moreover, hydrazone derivatives have excellent coordination properties to form complex with metal ions, especially Fe^{3+} and Ni^{2+}, leading to block the ion catalyzed physiological reaction or promote the absorption, transportation, distribution, and metabolism of drugs (Bernhardt et al. 2007). The cytotoxicities of synthesized benzylidene-hydrazone analogues were evaluated for against four human cancer cell lines, and their antioxidant effects using a DPPH assay. A computational study was also performed to predict the pharmacokinetic properties (ADME), MTIR (mutagenic, tumorigenic, irritant, and reproductive) toxicity profiles, and drug scores to identify the molecular features responsible for the cytotoxic

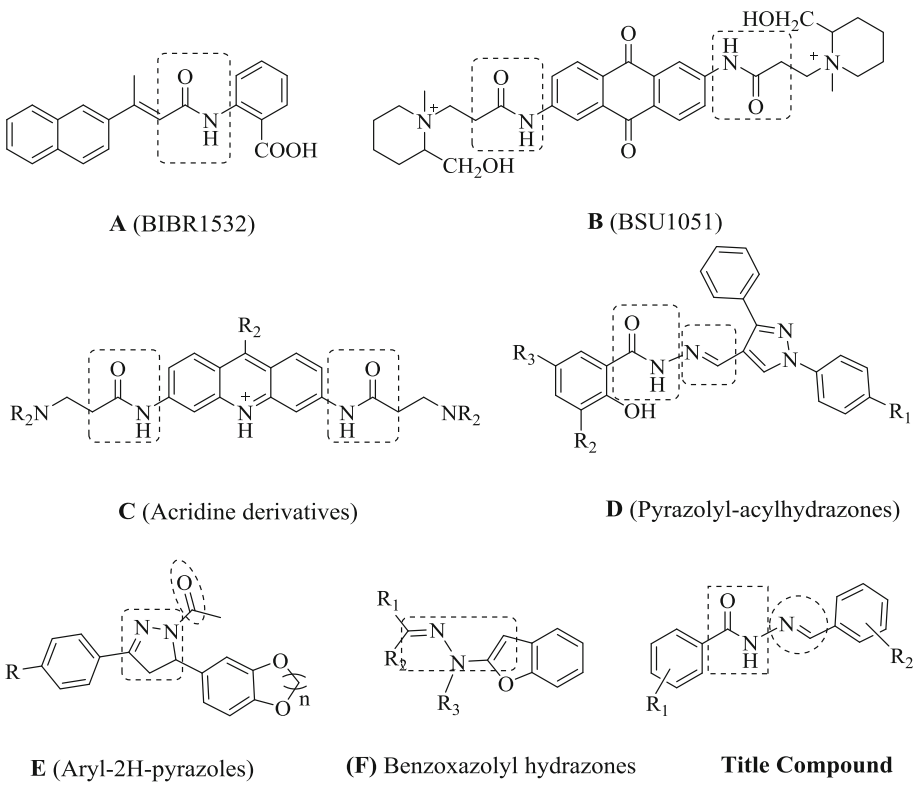

Fig. 1 Structures of several reported anticancer agents as telomerase inhibitors with pharmacodynamic scaffolds similar to the proposed benzylidene-hydrazone analogues

properties of these compounds. Furthermore, *in silico* screening was performed using the X-ray crystallographic structure of the catalytic subunit of telomerase to investigate compound binding affinity and modes at its active site. Exploiting the result of the present study, design and synthesis of more benzylidene-hydrazone derivatives are in progress to invent a potent anticancer agent as a telomerase inhibitor.

Materials and methods

General

The melting points were determined using a Stuart SMP3 apparatus, and were uncorrected. FT-IR spectra were obtained using a Bruker Tensor 37 spectrometer (Billerica, MA, USA) using KBr disc. NMR spectra were recorded using a Bruker 400 MHz (Billerica, MA, USA) spectrometer and TMS was used as the internal standard. Mass spectra were acquired using a Jeol JMS700 high-resolution mass spectrometer at the Korea Basic Science Center (Daegu, Korea). Elemental analyses (C, H, N) were performed on a Perkin Elmer 2400 II CHN elemental analyzer.

Chemistry

*General procedure for preparation of benzohydrazides (**2**)*

Benzohydrazide and 2-hydroxybenzohydrazide were prepared as we previously described (Alam and Lee 2015a). Briefly, methyl benzoate (13.6 g, 0.1 M) and methyl salicylate (15.2 g, 0.1 M), respectively were refluxed with hydrazine hydrate (12.5 g, 0.25 M) in approximately 100 cm^3 of ethanol for 3 h. The progress of the reaction was monitored by TLC (Silica gel $60F_{254}$, Merck, Germany). Precipitated benzohydrazides were filtered and recrystallized from an ethanol–water mixture. Mps and spectral data were compared with previously reported values to confirm structures.

*General procedure for the preparation of (E)-N′-benzylidene-hydrazide analogues (**3a–o**)*

Compounds **3a–o** were prepared as previously described (Alam and Lee 2015b). Briefly, benzohydrazides (**2**, 10 mM) in 30 cm^3 ethanol were added drop-wise into 20 mL of suitably substituted benzaldehydes (10 mM) in ethanol. The mixture was stirred and refluxed for 1.5–2.5 h. Reaction progress was monitored by TLC (Silica gel $60F_{254}$, Merck, Germany). After cooling reaction mixtures to ambient temperature, mixtures were filtered to give solid crude products, which were crystallized from ethanol yielding the pure compounds. All compounds except **3a**, **3c**, **3g**, **3h,** and **3m–o** are new (Alam and Lee 2015b) and their spectral and characterization data are included in the supplementary material.

*(E)-N′-(4-hydroxybenzylidene)benzohydrazide (**3b**)* Yield: 85 %, m.p. 267–268 °C (brown powder). IR (KBr) ν_{max} 3609 (OH), 3203 (NH), 2919 (CH), 1676 (C=O) cm^{-1}; ^{1}H NMR (DMSO-d_6, 400 MHz), δ: 7.02 (d, 2H, $J = 7.6$, Ar–H), 7.70–8.08 (m, 5H, Ar–H), 8.53 (s, 1H, CH), 8.67 (d, 2H, $J = 7.8$, Ar–H), 11.86 (s, 1H, NH); ^{13}C NMR (DMSO-d_6, 100 MHz), δ: 116.58 (C × 2), 126.17, 128.42 (C × 2), 129.30 (C × 2), 129.72 (C × 2), 132.45, 134.55, 148.99 (C=N), 160.31, 163.71 (C=O); EIMS *m/z* (%) 240 (M^+, 30), 110 (100); Anal. calcd. for $C_{14}H_{12}N_2O_2$: C, 69.99; H, 5.03; N, 11.66. Found: C, 70.08; H, 5.09; N, 11.71.

*(E)-N′-(2,4-dihydroxybenzylidene)benzohydrazide (**3d**)* Yield: 87 %, m.p. 246–247 °C (brown powder). IR (KBr) ν_{max} 3399 (OH), 3252 (NH), 2919 (CH), 1662 (C=O) cm^{-1}; ^{1}H NMR (DMSO-d_6, 400 MHz), δ: 6.32–6.39 (m, 2H, Ar–H), 7.28–7.33 (m, 1H, Ar–H), 7.49–7.60 (m, 3H, Ar–H), 7.90–7.94 (m, 2H, Ar–H), 8.51 (s, 1H, CH), 11.49 (s, 1H, NH); ^{13}C NMR (DMSO-d_6, 100 MHz), δ: 109.12, 112.37, 122.74, 127.93, 128.45 (C × 2), 129.33 (C × 2), 132.52, 134.49, 148.91 (C=N), 150.97, 152.64, 163.87 (C=O); EIMS *m/z* (%) 256 (M^+, 40), 137 (100); Anal. calcd. for $C_{14}H_{12}N_2O_3$: C, 65.62; H, 4.72; N, 10.93. Found: C, 65.69; H, 4.77; N, 11.01.

*(E)-N′-(2,4-dimethoxybenzylidene)benzohydrazide (**3e**)* Yield: 88.5 %, m.p. 178–179 °C (white powder). IR (KBr) ν_{max} 3183 (NH), 3008 (CH), 1725 (C=O) cm^{-1}; ^{1}H NMR (DMSO-d_6, 400 MHz), δ: 3.80 (s, 3H, –OCH_3), 3.88 (s, 3H, –OCH_3), 6.38–6.47 (m, 2H, Ar–H), 7.40–7.87 (m, 6H, Ar–H), 8.54 (s, 1H, CH), 10.91 (s, 1H, NH); ^{13}C NMR (DMSO-d_6, 100 MHz), δ: 56.31 (CH_3), 56.65 (CH_3), 99.16, 107.26, 116.04, 127.57, 128.42 (C × 2), 129.27 (C × 2), 132.42, 134.46, 144.20 (C=N), 160.04, 161.31, 163.59 (C=O); EIMS *m/z* (%) 284 (M^+, 15), 163 (100); Anal. calcd. for $C_{16}H_{16}N_2O_3$: C, 67.59; H, 5.67; N, 9.85. Found: C, 67.68; H, 5.72; N, 9.89.

*(E)-N′-(3,4-dihydroxybenzylidene)benzohydrazide (**3f**)* Yield: 91 %, m.p. 208–209 °C (white powder). IR (KBr) ν_{max} 3660 (OH), 3309 (NH), 2904 (CH), 1720 (C = O) cm^{-1}; ^{1}H NMR (DMSO-d_6, 400 MHz), δ: 6.82–7.01 (m, 2H, Ar–H), 7.31 (s, 1H, Ar–H), 7.57–7.61 (m, 3H, Ar–H), 7.93-7.98 (d, 2H, $J = 7.6$ Hz, Ar–H), 8.32 (s, 1H, CH), 11.68 (s, 1H, NH); ^{13}C NMR (DMSO-d_6, 100 MHz), δ: 113.55, 116.43, 121.47, 126.63, 128.39 (C × 2), 129.30 (C × 2), 132.42, 134.55, 146.60 (C=N), 148.88, 149.21,

163.68 (C=O); EIMS *m/z* (%) 256 (M^+, 35), 105 (100); Anal. calcd. for: $C_{14}H_{12}N_2O_3$: C, 65.62; H, 4.72; N, 10.93. Found: C, 65.71; H, 4.78; N, 11.00.

(E)-N′-(4-Hydroxy-3,5-dimethoxybenzylidene)benzohydrazide ***(3i)*** Yield: 90 %, m.p. 227–228 °C (white powder). IR (KBr) ν_{max} 3536 (OH), 3224 (NH), 2904 (CH), 1710 (C=O) cm^{-1}; ^{1}H NMR (DMSO-d_6, 400 MHz), δ: 3.83 (s, 6H, OCH_3), 6.99 (s, 2H, Ar–H), 7.49–7.60 (m, 3H, Ar–H), 7.88–7.93 (m, 2H, Ar–H), 8.34 (s, 1H, CH), 11.73 (s, 1H, NH); ^{13}C NMR (DMSO-d_6, 100 MHz), δ: 56.89 (CH_3 × 2), 105.51 (C × 2), 125.42, 128.42 (C × 2), 129.36 (C × 2), 132.52, 134.40, 138.80, 148.99 (C × 2), 149.40 (C=N), 163.99 (C=O); EIMS *m/z* (%) 300 (M^+, 22), 105 (100); Anal. calcd. for $C_{16}H_{16}N_2O_4$: C, 63.99; H, 5.37; N, 9.33. Found: C, 64.10; H, 5.42; N, 9.39.

(E)-N′-(2,4,6-trihydroxybenzylidene)benzohydrazide ***(3j)*** Yield: 81 %, mp 260–261 °C (deep-red powder). IR (KBr) ν_{max} 3610 (OH), 3182 (NH), 2912 (CH), 1710 (C=O) cm^{-1}; ^{1}H NMR (DMSO-d_6, 400 MHz), δ: 5.85 (s, 2H, Ar–H), 7.53 (d, 2H, $J = 7.6$ Hz, Ar–H), 7.92 (d, 2H, $J = 7.6$ Hz, Ar–H), 8.81 (s, 1H, Ar–H), 8.83 (s, 1H, CH), 11.10 (s, OH), 11.90 (s, 1H, NH); ^{13}C NMR (DMSO-d_6, 100 MHz), δ: 95.25 (C × 2), 99.92, 128.39 (C × 2), 129.39 (C × 2), 132.63, 133.76, 147.72 (C=N), 160.61 (C × 2), 162.44, 163.15 (C=O); EIMS *m/z* (%) 272 (M^+, 20), 105 (100); Anal. calcd. for $C_{14}H_{12}N_2O_4$: C, 61.76; H, 4.44; N, 10.29. Found: C, 61.83; H, 4.50; N, 10.37.

(E)-2-Hydroxy-N′-(4-hydroxybenzylidene)benzohydrazide ***(3k)*** Yield 86 %, m.p. 269–270 °C (white powder). IR (KBr) ν_{max} 3490 (OH), 3212 (NH), 2909 (CH), 1718 (C=O) cm^{-1}; ^{1}H NMR (DMSO-d_6, 400 MHz), δ: 6.45–7.84 (m, 8H, Ar–H), 8.45 (1H, s, N=CH), 11.25 (s, 1H, NH); ^{13}C NMR (DMSO-d_6, 100 MHz), δ: 116.61 (C × 2), 117.81, 118.37, 125.96, 127.51, 129.27, 130.97 (C × 2), 131.75, 146.60 (C=N), 160.18, 161.13, 165.78 (C=O); EIMS *m/z* (%) 256 (M^+, 35), 137 (100); Anal. calcd. for $C_{14}H_{12}N_2O_3$: C, 65.62; H, 4.72; N, 10.93. Found: C, 65.66; H, 4.62; N, 10.95.

(E)-2-hydroxy-N′-(2-hydroxybenzylidene)benzohydrazide ***(3l)*** Yield 89 %, m.p. 274–275 °C (brown powder). IR (KBr) ν_{max} 3569 (OH), 3192 (NH), 2949 (CH), 1680 (C=O) cm^{-1}; ^{1}H NMR (DMSO-d_6, 400 MHz), δ: 6.35–7.90 (m, 8H, Ar–H), 8.70 (s, 1H, =CH–), 11.27, (s, 1H, NH); ^{13}C NMR (DMSO-d_6, 100 MHz), δ: 116.52, 117.31, 118.16, 119.50, 119.89, 120.29, 129.45, 130.30, 132.52, 134.85, 149.78 (C=N), 158.37, 159.86, 165.38 (C=O); EIMS *m/z* (%) 256 (M^+, 40), 105 (100); Anal. calcd. for $C_{14}H_{12}N_2O_3$: C, 65.62; H, 4.72; N, 10.93. Found: C, 65.68; H, 4.73; N, 10.89.

Biological evaluation

The DPPH free radical-scavenging activities and cytotoxicities were assayed using the Blois (Blois 1958) and the SRB (sulforhodamine-B) method (Skehan et al. 1990), respectively and description of the assays are included in the supplementary material.

Computational studies

The details of the computational studies e.g. drug-likeness and ADME properties, *in silico* screening and conformational analysis are described as supplementary material.

Results and discussion

Synthesis and characterisation

The desired benzylidene-hydrazone analogues (**3a–o**) were prepared using a straightforward two step reactions, as presented in Scheme 1. The structures of the synthesized compounds were elucidated by FT-IR, ^{1}H NMR, ^{13}C NMR, mass spectroscopy, and elemental analyses. The FT-IR spectra of compounds **3a–o** showed absorption bands in the 3430–3660 and 3174–3309 cm^{-1} regions resulting from –OH and –NH– stretch, respectively, the >C=O stretch absorption band was observed at 1648–1667 cm^{-1}. The ^{1}H NMR spectra of compounds **3a–o** showed singlet protons at 8.13–8.70 and 10.27–11.94 ppm corresponding to the –CH=N– and =N–NH– protons, respectively. Aromatic protons and the protons of other functional group produced bands in accord with substitution patterns. In the ^{13}C NMR spectra, azomethine (C=N) and carbonyl (C=O) carbon showed two characteristics peaks around 144.20–149.78 and 163.15–165.78 ppm, respectively. The aromatic and methoxyl functional group carbons were assigned in the usual way. The previously reported crystal structure of compounds **3g** and **3m** (Alam and Lee 2015a, b) confirmed the *E*-configuration around the azomethine functional group (–CH=N–NHCO–) of benzylidene hydrazone analogues. The EI-MS spectra of **3a–o** showed molecular ion peaks with intensities of 22–35 %. FT-IR, ^{1}H-NMR, ^{13}C-NMR and mass spectrometric data together with elemental analyses data of newly synthesized compounds are summarized in ''Experimental'' part.

Anticancer activity

The in vitro cytotoxicities of benzylidene-hydrazone analogues (**3a–o**) were examined in four human cancer cell lines, namely, a lung cancer (A549), an ovarian cancer (SK-OV-3), a skin cancer (SK-MEL-2), and a colon cancer

Scheme 1 The synthesis of novel (*E*)-*N*′-benzylidenebenzohydrazide analogues

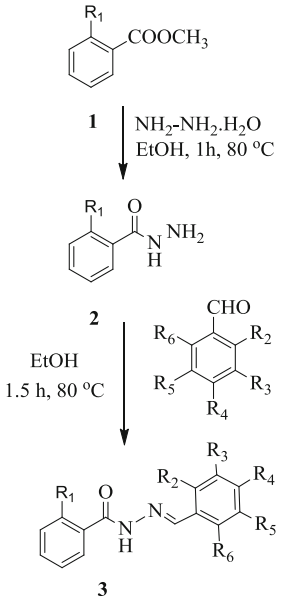

Comp.	R_1	R_2	R_3	R_4	R_5	R_6
3a	H	H	H	H	H	H
3b	H	H	H	OH	H	H
3c	H	H	H	OCH_3	H	H
3d	H	OH	H	OH	H	H
3e	H	OCH_3	H	OCH_3	H	H
3f	H	H	OH	OH	H	H
3g	H	H	OCH_3	OH	H	H
3h	H	H	OCH_3	OCH_3	H	H
3i	H	H	OCH_3	OH	OCH_3	H
3j	H	OH	H	OH	H	OH
3k	OH	H	H	OH	H	H
3l	OH	OH	H	H	H	H
3m	H	H	H	Cl	H	H
3n	H	H	H	$N(CH_3)_2$	H	H
3o	H	CHO	H	H	H	H

cell line (HCT15). Cytotoxic potencies were evaluated by measuring inhibitions of net cell proliferation (measured as percentages of controls) after incubation for 48 h using the SRB (sulforhodamine-B) method. Doxorubicin, a positive control is well-known telomerase inhibitor (Lanvers-Kaminsky et al. 2005; Yoon et al. 2003). As presented in Table 1, of the fifteen compounds, compound **3e** showed greatest cytotoxic activity against all four cancer cell lines, followed by compounds **3l**, **3d**, and **3n**. In particular, compound **3e** exhibited > 17 and 3 times greater activity against HCT15 (IC_{50} 0.05 μM) and SK-OV-3 (IC_{50} 0.024 μM), but less activity against A549 (IC_{50} 0.12 μM) and SK-MEL-2 (IC_{50} 0.097 μM) than doxorubicin (IC_{50} 0.872, 0.074, 0.021 and 0.001 μM, respectively), a potent anticancer drug.

Our structure–activity relationship study revealed that the cytotoxic activities of the fifteen benzylidene hydrazone analogues were significantly influenced by the positions and natures of groups on the phenyl rings. Compound **3a**, which has no substituent on its phenyl rings, had weak or very weak activity against the four human cancer lines as determined by the SRB method. However, introducing a methoxy group at the *ortho*- and *para*-positions of the benzylidene phenyl ring of **3a** to produce **3e** drastically increased cytotoxicity. In particular, the cytotoxicities of **3e** against ovarian and colon cancer cells were higher than those of doxorubicin. However, a shift in the position of the methoxy group or OH group at the *ortho*-position of the benzylidene phenyl ring in **3e** or **3d** to the *meta*-position in **3h** or **3f**, respectively, appreciably reduced cytotoxic effects, and **3i** possessing methoxy groups at both *meta*-positions led to least activity against all cell lines. These results suggest that the *ortho*- and *para*-positions in the benzylidene phenyl ring importantly determine cytotoxicity. When both methoxy groups in **3e** were replaced by OH

Table 1 In vitro cytotoxicity data of the 15 benzylidene-hydrazone analogues (**3a–o**) against selected human cancer cell lines

Comp.	IC_{50} values/μM[a]			
	A549[b]	SK-OV-3[c]	SK-MEL-2[d]	HCT15[e]
3a	470.0	125.0	176.0	402.0
3b	>500.0	145.0	128.0	>500.0
3c	498.0	76.74	110.0	193.0
3d	5.71	4.26	6.84	7.03
3e	0.12	0.024	0.097	0.05
3f	62.19	31.57	38.16	57.34
3g	435.0	>500.0	235.0	395.0
3h	167.0	63.25	51.44	59.76
3i	>500.0	>500.0	270.0	>500.0
3j	498.0	>500.0	325.0	333.0
3k	37.51	34.46	36.14	47.33
3l	2.25	1.50	2.41	1.96
3m	93.51	40.34	36.17	58.96
3n	17.14	8.27	8.12	7.86
3o	>500.0	480.0	320.0	>500.0
Doxorubicin	0.021	0.074	0.001	0.872

[a] IC_{50} values were obtained using dose response curves by nonlinear regression using a curve fitting program, OriginPro 7.5

[b] Human lung cancer

[c] Human ovarian cancer

[d] Human skin cancer

[e] Human colon cancer

to produce **3d**, cytotoxicities against all cell lines substantially were decreased, although **3d** was also potent. Whereas, cytotoxicity of **3l** with an OH group at the *ortho*-positions of both phenyl rings was much greater than that of **3d** against all cancer cells. Furthermore, an OH group at the *meta*-position (as in **3f**) significantly reduced activity versus **3d** or **3l**. The above findings indicate that the substituent position in the phenyl ring plays more crucial role than the kinds of the substituent, that is, the *ortho*-substitution led to potent activity (cf. **3e** > **3l** > **3d**), whereas the *meta*-substitution decreased activity greatly (cf. **3f–i**). But a methoxy substituent with moderate electron-donating ability more enhances cytotoxicity than an OH group, which has a stronger electron-donating effect (cf. **3e** > **3d**). Notably, when an electron-withdrawing group was present on the benzylidene phenyl ring (e.g. **3o**), the cytotoxic effect almost disappeared. These structure–activity relationships led us to speculate that an optimum electron density on the benzylidene phenyl ring of hydrazone analogues might determine their cytotoxic activities.

Antioxidant activity

The synthesized benzylidene-hydrazone analogues (**3a–o**) were also evaluated for their free radical-scavenging activity using DPPH. As listed in Table 2, all compounds exhibited antioxidant activity with a wide range of IC_{50} values (0.60–264 μM). Compound **3f** with two OH groups at the *meta*- and *para*-positions of the benzylidene ring displayed greatest free radical-scavenging activity (IC_{50} = 0.60 μM), and this was higher than that of ascorbic acid (IC_{50} = 0.87 μM). Other potent compounds (**3i** > **3g**) possessed OH group at the *para*-position and a methoxy group at the *meta*-position. Methoxy group substitution in **3f**, instead of OH substitution, decreased activity drastically (cf. **3h**). These results suggest that the polar OH group at the *para*-position of the benzylidene phenyl ring is essential for DPPH scavenging activity.

Table 2 DPPH radical scavenging activities of the benzylidene-hydrazone analogues (**3a–o**)

Comp. no	IC_{50} values/μM	Comp. no	IC_{50} values/μM
3a	360[a]	**3i**	0.99
3b	2.49	**3j**	3.67
3c	133.71	**3k**	36.58
3d	8.19	**3l**	9.55
3e	12.31	**3m**	264[a]
3f	0.60	**3n**	11.0[a]
3g	1.30	**3o**	114[a]
3h	164[a]	Ascorbic acid	0.87

[a] Alam and Lee (2015a)

However, compounds having OH group at the *ortho* position (**3j** > **3d** > **3l**) showed much weaker activity than the potent compounds (e.g. **3f** > **3i** > **3g** > **3b**). Furthermore, compounds possessing an electron-withdrawing group (**3o**) or a strong electronegative group (e.g. **3m**) exhibited poor activity. The above structure–activity relationship study led us to hypothesize that the position of substituents (particularly the OH group) on the benzylidene phenyl ring of hydrazone analogues plays a key role in determining antioxidant activity.

ADME and drug-likeness properties

Absorption, distribution, metabolism, and excretion (ADME) and drug-likeness properties of compounds **3a–o** have been calculated and are presented in Table 3. Moreover, the calculated toxicity effects and drug scores of the synthesized compounds and of doxorubicin and BIBR1532 are also presented in Fig. 2. The discussion of these results has been provided as a "supplementary material". The results of ADME and drug-likeness properties together with the calculated toxicity effects and drug scores of synthesized compounds suggest that benzylidene-hydrazone analogues (**3a–o**) have good drug-likeness properties.

In silico screening

To predict the binding affinity and mode of the benzylidene-hydrazone analogues, the most active (**3d, 3e, 3l** and **3n**) and moderately active (**3f, 3h, 3k** and **3m**) compounds were docked into the catalytic subunit of telomerase (Gillis et al. 2008) using AutoDock tools (Morris et al. 2009) 1.5.6 and AutoDock Vina in PyRx 0.8 software (Trott and Olson 2010). Telomerase is an enzyme, and its active site is composed of two major components, that is, the human telomerase RNA (hTR) and the human telomerase reverse transcriptase (hTERT) catalytic subunit, and also includes many associated protein that are important for proper function. It is revealed that hTERT is the attractive target for the discovery of telomerase inhibitors (Gillis et al. 2008; Levelle et al. 2000). The crystal structure of telomerase reverse transcriptase (TERT) catalytic subunit was retrieved from the Protein Data Bank (PDB ID: 3DU6). *In silico* screening results are summarized in Table 4. These studies revealed that the benzylidene-hydrazones (**3d-f**, **3h** and **3k–n**) bind to the active site of telomerase (Luo et al. 2013; Xing et al. 2014) by various hydrophobic, electrostatic, covalent, and Van der Wall's interactions. Binding modes and the different types of interactions found for most active compound **3e** is shown in Fig. 3, and docking models for compounds **3d**, **3f**, **3h,** and **3k–n** have been provided as supporting data (Figs. S1–S7, respectively).

Table 3 Calculated Lipinski's rule of five, Veber's rule, and solubility and absorption parameters of the benzylidene-hydrazone analogues (**3a–o**) and doxorubicin

Comp.	Lipinski's violations (≤1)	Based on Lipinski rule				Based on Veber rule		LogS[g]	%ABS[h]
		HBA[a] (≤10)	HBD[b] (≤5)	ClogP[c] (≤5)	MW[d] (≤500)	NROTB[e] (≤10)	TPSA[f] (≤140 Å^2)		
3a	0	3	1	3.099	224.263	3	41.462	−3.72	94.70
3b	0	4	2	2.619	240.262	3	61.69	−3.42	87.72
3c	0	4	1	3.155	254.289	4	50.696	−3.74	91.51
3d	0	5	3	2.536	256.261	3	81.918	−3.13	80.74
3e	0	5	1	3.14	284.315	5	59.93	−3.76	88.32
3f	0	5	3	2.13	256.261	3	81.918	−3.13	80.74
3g	0	5	2	2.438	270.288	4	70.924	−3.44	84.53
3h	0	5	1	2.745	284.315	5	59.93	−3.76	88.32
3i	0	6	2	2.454	300.314	5	80.158	−3.46	81.35
3j	0	6	4	2.452	272.26	3	102.146	−2.83	73.76
3k	0	5	3	2.56	256.261	3	81.918	−3.13	80.74
3l	0	5	3	3.528	256.261	3	81.918	−3.13	80.74
3m	0	3	1	3.777	258.708	3	41.462	−4.46	94.70
3n	0	4	1	3.201	267.332	4	44.70	−3.76	93.58
3o	0	4	1	2.841	252.273	4	58.533	−4.04	88.81
Doxorubicin	2	11	7	0.879	541.553	5	196.844	−5.32	41.09

[a] Number of hydrogen-bond acceptors

[b] Number of hydrogen-bond donors

[c] Calculated octanol/water partition coefficient

[d] Molecular weight

[e] Number of rotatable bonds

[f] Molecular polar surface area

[g] Solubility parameter

[h] Percentage absorption

Comp.	Toxicity effects			
	M	T	I	R
3a	Low	Low	Low	Low
3b	Low	Low	Low	Low
3c	Low	Low	Low	Low
3d	Low	Low	Low	Low
3e	Low	Low	Low	Low
3f	Low	Low	Low	Low
3g	Low	Medium	Low	Low
3h	Low	Low	Low	Low
3i	Low	Low	Low	Low
3j	Low	Low	Low	Low
3k	Low	Low	Low	Low
3l	Low	Low	Low	Low
3m	Low	Low	Low	Low
3n	Low	High	Low	Low
3o	Low	Low	Medium	High
Doxorubicin	Low	Low	High	Low
BIBR1532	Low	Low	Medium	Medium

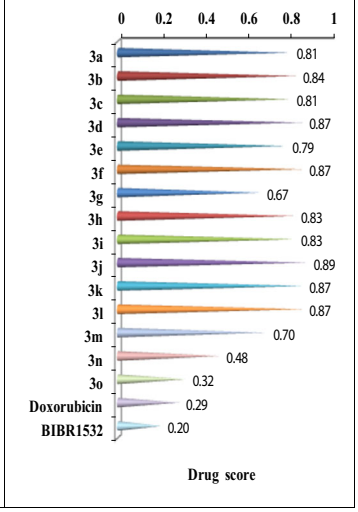

Fig. 2 Toxicity profiles (*left*) and drug scores (*right*) of the benzylidene-hydrazone analogues (**3a–o**), and of the anticancer agents doxorubicin and BIBR1532 (*M* mutagenic, *T* tumorigenic, *I* irritant, *R* reproductive)

Table 4 Docking results of the synthesized benzylidene-hydrazone analogues

Comp.	Binding energy (E/kJ mol^{-1})	H-bonding residues (ligands functional group)	Bond distance (Å)	No of H-bonds
3d	−32.24	ILE338 (>C=O), PHE329 (–OH)	2.72, 2.26	2
3e	−47.31	LEU419(>C=O), ARG592(–OCH_3)	2.25, 2.14	2
3f	−25.96	LYS392(>C=O), PHE443(–OH)	1.95, 2.12	2
3h	−24.28	ARG592(–OCH_3)	2.26	1
3k	−29.31	–	–	0
3l	−37.26	GLU386(–OH)	2.13	1
3m	−24.70	–	–	0
3n	−26.38	GLU386 (–NH)	2.83	1

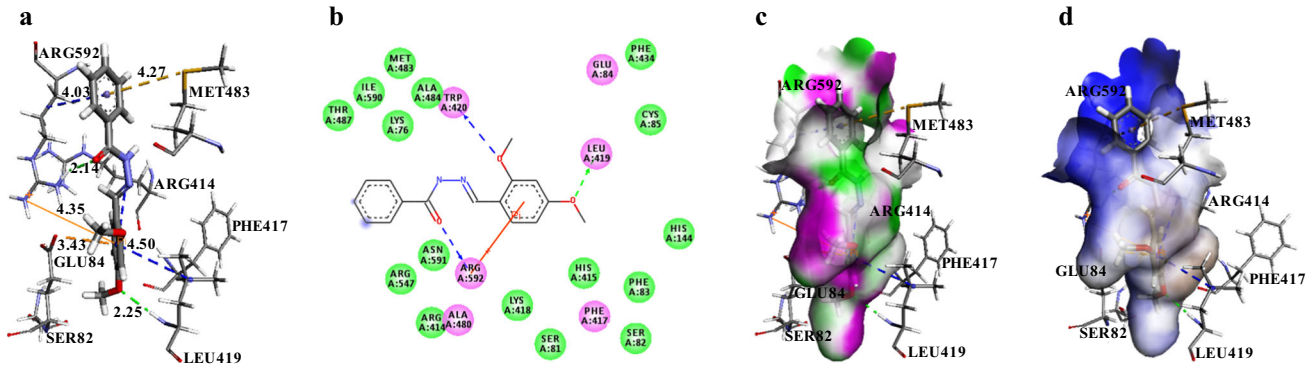

Fig. 3 **a** Binding of compound **3e** into telomerase (Protein Data Bank entry: 3DU6). The *green dotted lines* show the hydrogen bond, the *blue dotted lines* show π-alkyl interactions, and the *yellow dotted lines* show π-cation, π-pi, and π-sulfur interactions. **b** 2D ligand interaction diagram with telomerase using Discovery Studio program with the essential amino acid residues at the binding site are tagged in *circles*. The *purple circles* show the amino acids which involve in electrostatic and covalent interactions and the *green circles* show the amino acids which participate in the van der Waals interactions. **c** Hydrogen bond interaction showing donor (*pink*) and acceptor surfaces (*green*). **d** Hydrophobic interaction showing hydrophobic surface (*brown*)

The most active compounds, **3e** and **3l**, had low binding energies of −47.31 and −37.26 kJ mol^{-1}, respectively, which were lower than those of the moderately active compounds **3h** (−24.28 kJ mol^{-1}) and **3m** (−24.70 kJ mol^{-1}). This result indicates that compounds **3e** and **3l** bind more tightly (Figs. 3 and S5, respectively) to the active site of telomerase to that of **3h** and **3m** (Figs. S3 and S6, respectively) due to hydrogen bonding, hydrophobic, and van der Waal's interactions. In addition to hydrogen bonding (Table 4), **3d–f**, **3h** and **3k–n** exhibited electrostatic π-cation interactions with LYS225 (distance: 3.84 Å), ARG 592 (distance: 4.35 Å), LYS416 (distance: 3.73 Å), ARG592 (distance: 5.09 Å), GLU84 (distance: 3.74 Å), TYR577 (distance: 5.31 Å), LYS 584 (distance: 3.90 Å), and ARG402 (distance: 5.33 Å), respectively, and **3d**, **3e**, **3f**, and **3k** exhibited π-sulfur interactions with CYS233 (distance: 2.46 Å), MET483 (distance: 4.27 Å), CYS473 (distance: 5.95 Å), and MET483 (distance: 5.30 Å), respectively, and **3k** and **3l** exhibited π-sigma and π-pi interactions with THR487 (distance: 4.44 Å) and TYR577 (distance: 5.31 Å), respectively involving benzoyl- or benzylidene-phenyl rings. The following van der Waal's interactions were also observed between: **3d** and THR232, GLU236, PHE237, LEU332, PHE337, HIS339, and ARG340; **3e** and SER81, SER82, PHE83, CYS85, HIS144, ARG414, HIS415, LYS418, PHE434, MET483, ALA484, THR487, LYS576, ARG547, ILE590, and ASN591; **3f** and CYS390, THR403, LEU404, TRY405, and PHE417; **3h** and LYS76, GLU84, LEU419, TRP420, ALA484, MET483, and THR487; **3k** and SER81, ARG414, PHE417 and LEU419; **3l** and ILE93, ALA465, VAL573, ASP574, TYR577, PHE578 and LYS584; **3m** and PRO582, PRO388, GLU386, ILE387, ILE 393, ARG402, LEU404, and TYR577; **3n** and GLN388, ILE387, PRO388, ILE393, LEU404, ALA465, ASP574, LYS584, and TYR577 amino acid residues. The higher binding affinities of the most active compounds (**3d, 3e, 3l** and **3n**) could have been caused by additional π-sulfur and π-pi interactions with amino acid residues of the telomerase active site.

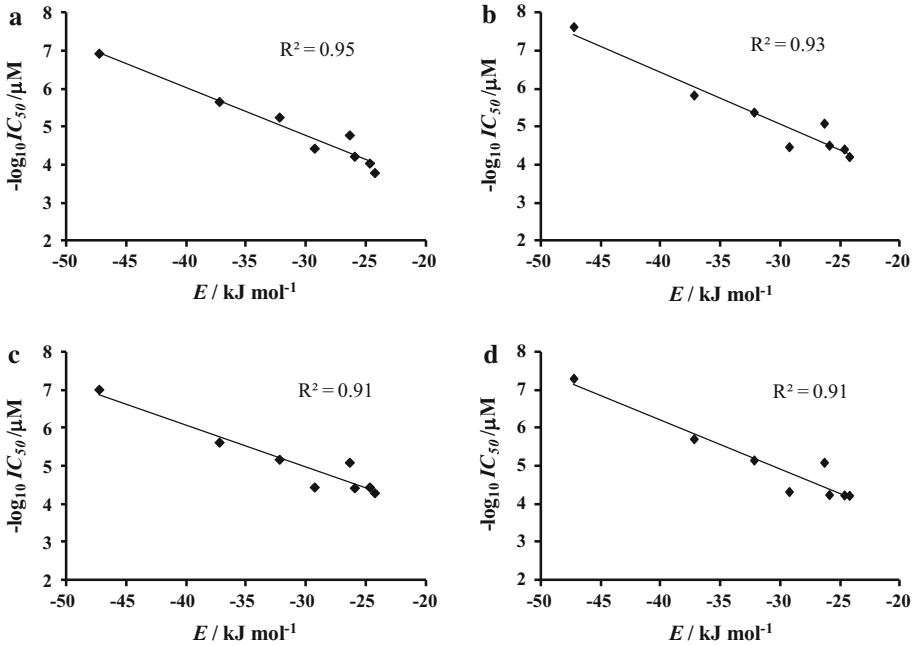

Fig. 4 Correlation between the total binding energy (*E*/ kJ mol^{-1}) with TERT protein catalytic subunit (PDB ID: 3DU6) determined by docking studies and the experimentally determined cytotoxic activity (pIC_{50}) of benzylidene-hydrazone analogues (**3d–f**, **3h** and **3k–n**) against **a** human lung cancer (A549), **b** human ovarian cancer (SK-OV-3), **c** human skin cancer (SK-MEL-2), and **d** human colon cancer (HCT15) cell lines

Finally, to validate the *in silico* screening results of benzylidene-hydrazone analogues into the TERT catalytic subunit, we examined the relationship between the total binding energies calculated by the docking studies and the experimentally determined cytotoxic potencies, pIC_{50} ($-\log_{10}IC_{50}$) values. A good correlations were observed between the binding energies of compounds **3d-f**, **3h** and **3k–n** and their corresponding pIC_{50} values against A549 (lung), SK-OV-3 (ovarian), SK-MEL-2 (skin), and HCT15 (colon) cancer cell lines (Fig. 4) with correlation coefficients (r^2) of 0.95, 0.93, 0.91, and 0.91, respectively. These findings suggest compounds **3e**, **3l**, and **3d** be considered leads to the development of anticancer agents as a telomerase inhibitor.

Conformational analysis

To gain a better understanding about the bioactive conformations of benzylidene-hydrazone analogues, we compared by the superimposition of the lowest energy optimized conformation and the docked conformation of the compounds **3d–f, 3h,** and **3k–n** and their superimpositions are presented in Fig. 5. The lowest energy conformer was obtained by the optimization with MM2 semi-empirical molecular orbital calculation (Allinger 1977). Analysis of these conformations indicates that the docked conformation of the higher active compounds e.g. **3d**, **3e**, and **3l** (Fig. 5a,b,f, respectively) are conformationally and energetically (data not shown) closer to their corresponding lowest energy optimized conformation except compound **3n**. As shown in Fig. 5h, the benzylidene phenyl ring of docked conformation of **3n** deviated more (69.73°), while the benzoyl phenyl ring showed minor deviation (5.31°) from its lowest energy optimized conformation. In contrast, the docked conformation of lower active compounds e.g. **3f**, **3h**, **3k** and **3m** (Fig. 5c–e, and g, respectively) are conformationally and energetically distinct to their corresponding lowest energy conformation. This result indicates that compounds **3f**, **3h**, **3k**, and **3m** require more energy to adopt docked conformation compare to that of compounds **3d**, **3e**, **3l**, and **3n**. Therefore, we could anticipate that compounds **3d**, **3e**, **3l**, and **3n** could bind more efficiently to the telomerase RT catalytic subunit to exert more potency compare to **3f**, **3h**, **3k**, and **3m.** The above consequence is consistent with the result of docking studies of benzylidene-hydrazone analogues.

Conclusion

We report the synthesis of novel benzylidene-hydrazone analogues as potential anticancer, and antioxidant agents. Using simple condensation reactions, fifteen benzylidene-hydrazone analogues were prepared and evaluated for cytotoxicity in four cancer cell lines and for DPPH free radical scavenging activity. Compound **3e** with two methoxy groups at *ortho*- and *para*-positions of the benzylidene phenyl ring was found to be most cytotoxic to all four cancer cell lines, and its activity against colon- and ovarian cancer cells was greater than that of doxorubicin. Furthermore, compound **3f** with two hydroxyl substituents at *meta*- and *para*-positions of the benzylidene phenyl ring

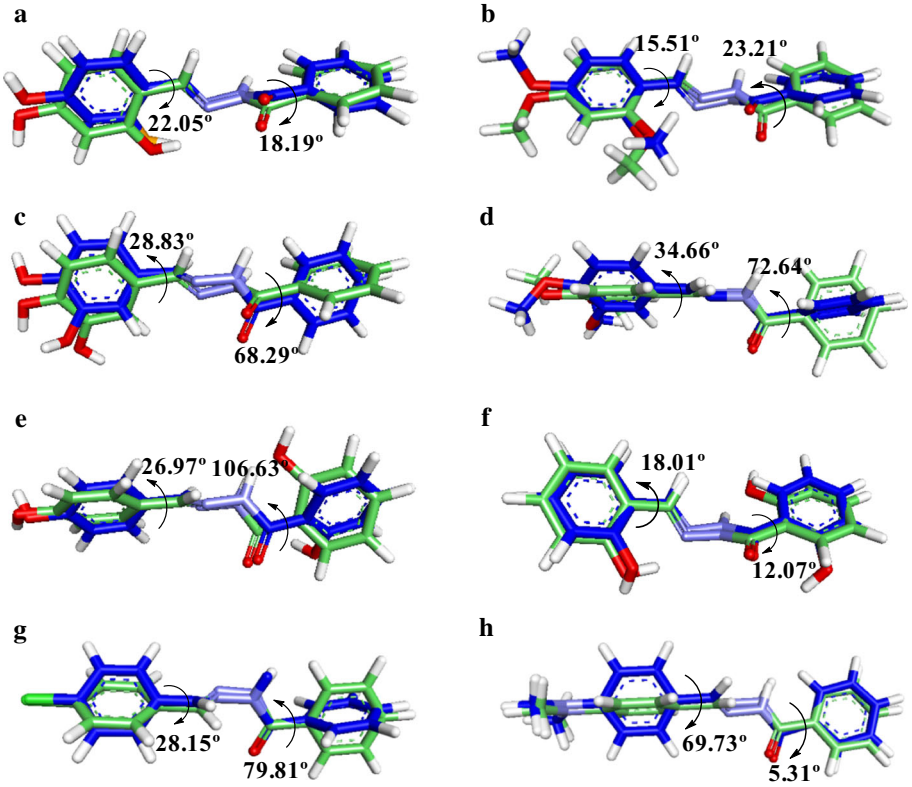

Fig. 5 Comparison between lowest energy conformation (*green color*) calculated by the semi-empirical molecular orbital MM2 method and docked conformation (*blue color*) of **3d** (**a**), **3e** (**b**), **3f** (**c**), **3h** (**d**), **3k** (**e**), **3l** (**f**), **3m** (**g**) and **3n** (**h**)

had greater DPPH radical scavenging activity than ascorbic acid. *In silico* screening studies were used to examine the probability of binding between these benzylidene-hydrazone analogues and the active site of telomerase, a unique ribonucleoprotein enzyme, and an important therapeutic target for anticancer agents. A good correlations were observed between the total binding energies of docked compounds and their corresponding cytotoxic potencies against A549 (lung), SK-OV-3 (ovarian), SK-MEL-2 (skin), and HCT15 (colon) cancer cell lines, which indicated benzylidene-hydrazones could be used for the development of new anticancer agents as a telomerase inhibitor. None of the fifteen analogues violated Lipniski's rule of five (ROF) or Veber's rule, and thus exhibited good drug-likeness and ADME properties and high drug scores. The above findings provided the theoretical basis for design and synthesis of novel benzylidene-hydrazone analogues as potential telomerase inhibitors.

References

Akelah A, Kenawy ER, Sherrington DC (1993) Agricultural polymers with herbicide/fertilizer function-III. Polyureas and poly (Schiff base)s based systems. Eur Polymer J 29:1041–1045

Alam MS, Lee DU (2015a) Quantum-chemical studies to approach the antioxidant mechanism of nonphenolic hydrazone Schiff base analogs: synthesis, molecular structure, hirshfeld and density functional theory analyses. Bull Korean Chem Soc 36: 682–691

Alam MS, Lee DU (2015b) Syntheses, crystal structure, Hirshfeld surfaces, fluorescence properties, and DFT analysis of benzoic acid hydrazone Schiff bases. Spectrochim Acta, Part A 145:563–574

Alam MS, Liu L, Lee DU (2011) Cytotoxicity of new 5-phenyl-4,5-dihydro-1,3,4-thiadiazole analogues. Chem Pharm Bull 59: 1413–1416

Alam MS, Choi JH, Lee DU (2012) Synthesis of novel Schiff base analogues of 4-amino-1,5-dimethyl-2-phenylpyrazol-3-one and their evaluation for antioxidant and anti-inflammatory activity. Bioorg Med Chem 20:4103–4108

Alam MS, Nam YJ, Lee DU (2013) Synthesis and evaluation of (Z)-2,3-diphenylacrylonitrile analogs as anti-cancer and anti-microbial agents. Eur J Med Chem 69:790–797

Allinger NL (1977) A hydrocarbon force field utilizing V1 and V2 torsional terms. J Am Chem Soc 99:8127–8134

Anouar EH (2014) A quantum chemical and statistical study of phenolic Schiff bases with antioxidant activity against DPPH free radical. Antioxidants 3:309–322

Bernhardt PV, Chin P, Sharpe PC, Richardson DR (2007) Hydrazone chelators for the treatment of iron overload disorders: iron coordination chemistry and biological activity. Dalton Trans 30:3232–3244

Blois MS (1958) Antioxidant determinations by the use of a stable free radical. Nature 455:1199–1200

Gillis AJ, Schuller AP, Skordalakes E (2008) Structure of the *Tribolium castaneum* telomerase catalytic subunit TERT. Nature 455:633–637

Hearn MJ, Cynamon MH, Chen MF, Coppins R, Davis J, Joo-On Kang H, Noble A, Tu-Sekine B, Terrot MS, Trombino D, Thai

M (2009) Preparation and antitubercular activities in vitro and in vivo of novel Schiff bases of isoniazid. Eur J Med Chem 44:4169–4178

Jain JS, Srivastava RS, Aggrawal N, Sinha R (2007) Synthesis and evaluation of schiff bases for anticonvulsant and behavioral depressant properties. Cent Nerv Syst Agents Med Chem 7:200–204

Lanvers-Kaminsky C, Winter B, Koling S, Frodermann B, Braun Y, Schaefer KL, Diallo R, Koenemann S, Wai D, Willich N, Poremba C (2005) Doxorubicin modulates telomerase activity in Ewing's sarcoma in vitro and in vivo. Oncol Rep 14:751–758

Levelle F, Riou JF, Laoui A, Mailliet P (2000) Telomerase: a therapeutic target for the third milleneum? Crit Rev Oncol Hematol 34:111–126

Luo Y, Zhang S, Qiu KM, Liu ZJ, Yang YS, Fu J, Zhong WQ, Zhu HL (2013) Synthesis, biological evaluation, 3D-QSAR studies of novel aryl-2H-pyrazole derivatives as telomerase inhibitors. Bioorg Med Chem Lett 23:1091–1095

Mishra P, Gupta PN, Shakya AK, Shukla R, Srimal RC (1995) Anti-inflammatory and diuretic activity of a new class of compounds-Schiff bases of 3-amino-2-methylquinazolin 4(3H)-ones. Indian J Physiol Pharmacol 39:169–172

Mohan M, Gupta MP, Chandra L, Jha NK (1988) Synthesis, characterization and antitumour properties of some metal(II) complexes of 2-pyridinecarboxaldehyde 2′-pyridyl hydrazone and related compounds. Inorg Chim Acta 151:61–68

Moorthy NSHN, Nuno SC, Maria JR, Pedro AF (2012) QSAR analysis of 2-benzoxazolyl hydrazone derivatives for anticancer activity and its possible target prediction. Med Chem Res 21: 133–144

Morris GM, Huey R, Lindstrom W, Sanner MF, Belew RK, Goodsell DS, Olson AJ (2009) AutoDock4 and AutoDockTools4: automated docking with selective receptor flexibility. J Comput Chem 30:2785–2791

Pascolo E, Wenz C, Lingner J, Hauel N, Priepke H, Kauffmann I (2002) Mechanism of human telomerase inhibition by BIBR1532, a synthetic, non-nucleosidic drug candidate. J Biol Chem 77:15566–15572

Rasras AJM, Al-Tel TH, Amal AF, Al-Qawasmeh RA (2010) Synthesis and antimicrobial activity of cholic acid hydrazone analogues. Eur J Med Chem 45:2307–2313

Read M, Harrison RJ, Romagnoli B, Tanious FA, Gowan SH, Reszka AP, Wilson WD, Kelland LR, Neidle S (2001) Structure-based design of selective and potent G quadruplex-mediated telomerase inhibitors. Proc Natl Acad Sci 98:4844–4849

Seigel RL, Miller KD, Jemal A (2015) Cancer statistics, 2015. CA Cancer J Clin 65:5–29

Skehan P, Streng R, Scudiero D, Monks A, McMahon J, Vistica D, Warren JT, Bokesch H, Kenney S, Boyd MR (1990) New colorimetric cytotoxicity assay for anticancer-drug screening. J Natl Cancer Inst 82:1107–1112

Sun-Waterhouse D, Chen J, Chuah C, Wibisono R, Melton LD, Laing W, Ferguson LR, Skinner MA (2009) Kiwifruit-based polyphenols and related antioxidants for functional foods: kiwifruit extract-enhanced gluten-free bread. Int J Food Sci Nutr 60:251–264

Supuran CT, Barboiu M, Luca C, Pop E, Brewster ME, Dinculescu A (1996) Carbonic anhydrase activators. Part 14. Syntheses of mono and bis pyridinium salt derivatives of 2-amino-5-(2-aminoethyl)- and 2-amino-5-(3-aminopropyl)-1,3,4-thiadiazole and their interaction with isozyme II. Eur J Med Chem 31:597–606

Tian FF, Jiang FL, Han XL, Xiang C, Ge YS, Li JH, Zhang Y, Li R, Ding XL, Liu Y (2010) Synthesis of a novel hydrazone derivative and biophysical studies of its interactions with bovine serum albumin by spectroscopic, electrochemical, and molecular docking methods. J Phys Chem B 114:14842–14853

Trott O, Olson AJ (2010) AutoDock Vina: improving the speed and accuracy of docking with a new scoring function, efficient optimization and multithreading. J Comput Chem 31:455–461

Xing M, Zhao TT, Ren YJ, Peng NN, Yang XH, Li X, Zhang H, Liu GQ, Zhang LR, Zhu HL (2014) Synthesis, biological evaluation, and molecular docking studies of pyrazolyl-acylhydrazone derivatives as novel anticancer agents. Med Chem Res 23:3274–3286

Yoon KA, Ku JL, Yang JO, Park JG (2003) Telomerase activity, expression of Bcl-2 and cell cycle regulation in doxorubicin resistant gastric carcinoma cell lines. Int J Mol Med 11:343–348

Zheng LW, Wu LL, Zhao BX, Dong WL, Miao JY (2009) Synthesis of novel substituted pyrazole-5-carbohydrazide hydrazone derivatives and discovery of a potent apoptosis inducer in A549 lung cancer cells. Bioorg Med Chem 17:1957–1962